

Koopman-Based Event-Triggered Control from Data

Zeyad M. Mana

Ayman M. Abdallah

Mohamed Ismail

Samir El Ferik

Abstract. Event-triggered Control (ETC) presents a promising paradigm for efficient resource usage in networked and embedded control systems by reducing communication instances compared to traditional time-triggered strategies. This paper introduces a novel approach to ETC for discrete-time nonlinear systems using a data-driven framework. By leveraging Koopman operator theory, the nonlinear system dynamics are globally linearized (approximately in practical settings) in a higher-dimensional space. We design a state-feedback controller and an event-triggering policy directly from data, ensuring exponential stability in Lyapunov sense. The proposed method is validated through extensive simulation experiments, demonstrating significant resource savings.

I INTRODUCTION

ETC is an implementation strategy in which the plant and its controller only exchange data when certain output- or state-related conditions are met. Event-triggered control seeks to reduce communication instances by concentrating on the real needs of the system, in contrast to traditional conservative time-triggered strategies that depend on fixed time intervals for communication. In situations where efficient use of resources is essential, like networked control systems and embedded systems, this paradigm has become more and more popular. ETC strategies, which offer improved system performance and resource savings in a variety of setups and control problems, have been developed in the literature thanks to the early results by Årzen in [1], Eker, Hagander, and Årzen in [2] and the work of Tabuada [3], and Heemels et al. [4].

In most of the current research, parametric state-

space models are the foundation of traditional control engineering, where the plant to be controlled must first be identified or modeled. These models make use of the data from the system (from the input and the output) and are frequently written down starting from physics first principles or architecturally constrained system identification techniques. But in cases when first-principles models are intricate or hard to derive, they can only be considered as approximate representations of real systems, which inevitably leads to modeling errors. These errors impede accurate control design and spread through the phases of analysis and implementation, affecting the overall performance of the system.

By excluding the demand for explicit system identification and instead of leveraging data gathered from open-loop simulations/experiments for any system control analysis and design, data-driven control techniques serve as a promising alternative. Several data-driven techniques for creating state feedback controllers and illustrating system dynamics have been shown in recent works, such as those by da Silva et al. [5], and De Persis and Tesi [6]. These techniques greatly streamline the control design process and do not require constantly exciting input data. There are also numerous applications of data-driven control in fields such as robotics [7], aerospace [8], and power systems [9]. Other methods, when the model is completely unknown, such as SINDy [10] can be utilized to firstly get a nonlinear representation of the dynamics of the system. For example, this approach is applied to model the dynamics of: i) quadrotors' [11], ii) disease [12], iii) optics communication systems [13], iv) chemical processes [14], v) and also robotics applications [15].

However, an alternative option in the situation, when first principles or system identification techniques fail, would be to construct the controller directly using the input, state, and output data that are now accessible. This approach is known as direct data-driven control [16]–[18]. Although the literature is full of data-driven techniques for control, only a limited number of techniques exist in the current literature [19]–[21] for data-driven event-based control, particularly for nonlinear systems. There exists, therefore, a profound demand for comprehensive data-driven event-based control meth-

Z. M. Manaa, A. M. Abdallah, and M. Ismail are with the Department of Aerospace Engineering, King Fahd University of Petroleum and Minerals (KFUPM), Dhahran, Saudi Arabia. Also with the Interdisciplinary Research Center for Aviation and Space Exploration. S. El Ferik is with the Department of Control and Instrumentation Engineering, KFUPM. Also with the Interdisciplinary Research Center for Smart Mobility and Logistics.

This work is supported by the Interdisciplinary Research Center for Aviation and Space Exploration (IRC-ASE) at KFUPM under project INAE2401.

This work was carried out during the stay of Z. M. Manaa at KFUPM.

ods tailored for general nonlinear systems, particularly applicable to discrete-time systems in our case. In many cases, it is appropriate and feasible to formulate the control and triggering conditions as data-dependent Linear Matrix Inequality (LMI). Given that most of the existing literature on ETC is well developed for Linear Time Invariant (LTI) systems, we aim to globally linearize nonlinear systems by increasing the dimensional space in which they reside.

This is not totally a new idea, as Koopman and von Neumann [22], [23] in 1930s presented a trade-off between the nonlinear nature of dynamical systems and infinite dimensional representation of the same nonlinear system but it will look linear in the lifted space. Another resurgence of attention in mid 2000s in the work of Mezić and Banaszuk [24], [25] has led to new applications and studies using the idea in many fields including, robotics, fluid dynamics, epidemiology, [26]–[34] and many other fields due to the intersection between data science and the easy-to-access computational domain.

We consequently propose Koopman Operator-Based Event-Triggered Control (KOETC), a technique inspired by Koopman Operator (KO) to acquire (approximately) global linear systems but in a higher dimensional space. Afterwards, we design the controller and the triggering policy for ETC for discrete-time linear systems directly from controlled system data, all together ensuring performance metrics (i.e. Lyapunov exponential stability).

I.A CONTRIBUTIONS

By combining Koopman operator theory with event-triggered control (ETC), this paper makes a contribution by introducing a Koopman-based approach to ETC for discrete-time nonlinear systems. Through the approximate global linearization of nonlinear dynamics made possible by this integration, the following direct, data-driven designs are made possible: i) An event-triggering policy minimizes resource consumption by updating control actions only when required, reducing communication instances; and ii) A state-feedback controller, which effectively stabilizes the system by utilizing the Koopman-lifted linear dynamics.

In comparison to time-triggered approaches, the KOETC framework reduces communication events in simulations while achieving stability in the Lyapunov sense.

The rest of this paper is structured to methodically construct and validate the suggested KOETC framework after the motivation and goals have been established. The preliminary information and notations that are necessary to comprehend our methodology are outlined in Section 2. In Section 3, the KOETC framework’s design

is examined in detail, including the triggering policy and data-driven controller. We provide simulation results in Section 4, which show how effective the approach is. The work’s conclusions and possible future research directions are finally provided in Section 5.

II PRELIMINARIES

II.A NOTATIONS AND BASIC DEFINITIONS

Let $\mathbb{Z}_{\geq 0} := \{0, 1, 2, \dots\}$ denote the set of nonnegative integers, and let $\mathbb{Z}_{>0} := \mathbb{Z}_{\geq 0} \setminus \{0\}$ denote the set of positive integers. We denote by \mathbb{R} the set of real numbers and use a similar notation as for \mathbb{Z} . The ℓ_2 norm of a vector (a finite sequence) is denoted by $\|\cdot\|$. The symbols I and 0 denote the identity matrix and the zero matrix, respectively. Given a symmetric matrix A , the notation $A \succ 0$ indicates that A is positive definite, while $A \succeq 0$ means that A is positive semi-definite. Similarly, $A \prec 0$ indicates that A is negative definite and $A \preceq 0$ means that A is negative semi-definite. For any matrix A , A^\top denotes the transpose of A . The symbol $\mathcal{N}(\mu, \sigma^2)$ represents a normal distribution with mean μ and variance σ^2 . Also, the symbol $\mathcal{U}(a, b)$ represents a normal distribution from the interval $[a, b]$. The symbol λ_i denotes an eigenvalue of a matrix.

II.B PROBLEM OVERVIEW

Consider the discrete time dynamical system

$$x_{k+1} = f(x_k, u_k), \quad (1)$$

where the state is $x_k \in \mathbb{R}^n$ and $u_k \in \mathbb{R}^m$ is the control input, each at time instant $k \in \mathbb{Z}_{\geq 0}$ with $n, m \in \mathbb{Z}_{>0}$, and f is a transition map such that $f : \mathbb{R}^n \times \mathbb{R}^m \mapsto \mathbb{R}^n$, generally nonlinear, and assumed to be unknown, and stabilizable.

We consider a scenario where the system in (1) is connected to a controller via networked medium. Especially, the state readings are provided to the controller through a digital channel, and the controller has direct access to the actuators. The goal is to design a data-driven event-triggered state-feedback controller with gain $K \in \mathbb{R}^{m \times n}$ to stabilize the plant in (1) while abiding by a triggering policy that defines the instances $\{k_i\}_{i \in \mathcal{Z}}$ at which a transmission happens, with $\mathcal{Z} \subseteq \mathbb{Z}_{\geq 0}$. At the time instant $k = 0$, we consider a transmission happens, so that $k_0 = 0$. In our settings, the controller is updated only upon the violation of some well-defined triggering policy in contrary to the nominal Time-triggered Control (TTC). The sequence $\{k_i\}_{i \in \mathcal{Z}}$ leads to aperiodic updates of the controller. The controller then follows a zero-order

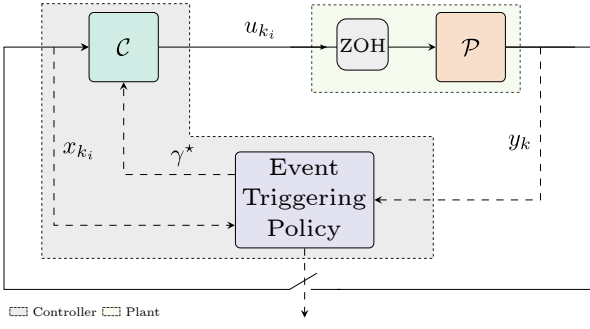


Figure 1: Block diagram visually providing representation that illustrates the core concept underlying ETC. It showcases various components and their interconnections, highlighting the essential principles and operational dynamics of the ETC framework.

hold implementation that takes the form of¹

$$u_k = Kx_{k_i}, \quad k \in [k_i, k_{i+1}), \quad (2)$$

The state error takes into account the provided controller's zero-order hold mechanism.

$$e_k = x_{k_i} - x_k, \quad (3)$$

which can be seen as the deviation between the current state and the last time an event (i) happened. We consider the relative thresholding metric and events occur with the violation of the condition

$$\|e_k\| \leq \gamma \|x_k\| \quad (4)$$

Where $\gamma > 0$ is a relative parameter for the thresholding policy. The policy in (4) is evaluated at every time instant k , and the control is updated only when the policy is violated. An overview of the ETC framework is shown in Fig. 1, where the plant \mathcal{P} represents (1), the controller \mathcal{C} represents the control law (2), and the event-triggering policy corresponds to (4).

II.C PERSISTENCE OF EXCITATION

Consider a carried out experiment for the system in (1) and its states and input data are recorded in the following way

$$\mathcal{D} := \{x_k, u_k : k \in [0, (T-1)] \cap \mathbb{Z}_{\geq 0}\},$$

¹To be more precise, the control law should be $u_k = K\xi(x_{k_i})$, $k \in [k_i, k_{i+1})$, where $\xi(x_{k_i})$ is the lifted state. Since we are introducing the vanilla event-triggered mechanism, we use the original state of the system for completeness. In our problem formulation, we adhere to $u_k = K\xi(x_{k_i})$, unless otherwise stated. The concept of lifting will be discussed in subsection III.A.

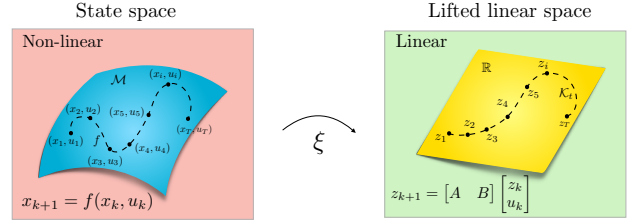


Figure 2: Illustration of the Koopman Operator: The red panel represents the generic nonlinear state-space. Conversely, the green panel represents the linear space.

where T is the final time of the experiment. Let set \mathcal{D} exists. Then, we define

$$U_0 := [u_0 \ u_1 \ \dots \ u_{T-1}] \in \mathbb{R}^{m \times T}, \quad (5a)$$

$$X_0 := [x_0 \ x_1 \ \dots \ x_{T-1}] \in \mathbb{R}^{n \times T}, \quad (5b)$$

$$X_1 := [x_1 \ x_2 \ \dots \ x_T] \in \mathbb{R}^{n \times T}. \quad (5c)$$

Assumption 1. Taking into account $T \geq n + m$, the matrix $\begin{bmatrix} X \\ U_0 \end{bmatrix}$ has full row rank. \square

Assumption 1 can be verified numerically for a given set \mathcal{D} . The results of Willems et al. [35] ensures, for discrete-time systems, the validity of assumption 1 as long as u is persistently exciting signal.

III FRAMEWORK

III.A KOOPMAN OPERATOR THEORY

Definition 1 (Koopman Operator (KO)). Consider the system given in (1). The KO \mathcal{K}_t is an infinite dimensional operator

$$\mathcal{K}_t \xi(x_k) = \xi \circ f(x_k), \quad (6)$$

acts on $\xi \in \mathcal{H} : \mathbb{R}^n \mapsto \mathbb{R}$, the observable functions of the state space, where \circ is the function composition. \square

The KO acts on the Hilbert space \mathcal{H} of all scalar measurement functions ξ and is by definition a linear operator—since for $\xi_1, \xi_2 \in \mathcal{H}$ and $\beta_1, \beta_2 \in \mathbb{R}$

$$\begin{aligned} \mathcal{K}_t(\beta_1 \xi_1, \beta_2 \xi_2) &= \beta_1 \xi_1 \circ f + \beta_2 \xi_2 \circ f \\ &= \beta_1 \mathcal{K}_t \xi_1 + \beta_2 \mathcal{K}_t \xi_2, \end{aligned} \quad (7)$$

An infinite-dimensional space \mathcal{H} of observable functions is used to represent a nonlinear system linearly using KO method [36]. This means that the dynamics are changed from nonlinear, finite-dimensional to linear, infinite-dimensional upon transitioning from the state-space model to the Koopman representation (see Fig. 2). However, we are interested in a finite-dimensional approximation of KO from a practical perspective. Several approximation methods are addressed in [37], [38].

To extend this analysis to controlled systems, there

exists several methods including [39], [40]. In [39], the authors treated the controlled system as uncontrolled while treating the input as a system parameter. On the other hand, Korda and Mezić [40] dealt with the controlled system in an extended state-space to account for control.

Here, the approach of [40] will be revisited in a short way. In particular, consider the system in (1). Let $\ell(\mathcal{U})$ be the space of all infinite vectors $u^\circ = \{u_k\}_{k=0}^\infty$ with the symbol $u_\circ \in \mathcal{U}$ and \mathcal{U} being an input space. We denote the left shift operator by \mathcal{G}^* (e.g., $\mathcal{G}^*u_k^\circ = u_{k+1}^\circ$). Also, define \mathcal{X} to be an extended state such that, $\mathcal{X} = [x_k \ u_k^\circ]^\top$. So, the system in (1) can be updated to be,

$$\mathcal{X}_{k+1} = \tilde{f}(\mathcal{X}) = \begin{bmatrix} f(x_k, u_0^\circ) \\ \mathcal{G}^*u_k^\circ \end{bmatrix}. \quad (8)$$

If $\tilde{\xi} \in \mathcal{H} : \mathbb{R}^n \times \mathbb{R}^m \mapsto \mathbb{R}$ be a new version of the predefined observable function, the Koopman operator $\mathcal{K}_t : \mathcal{H} \mapsto \mathcal{H}$ for the controlled system turns out to be,

$$\mathcal{K}_t \tilde{\xi}(\mathcal{X}) = \tilde{\xi} \circ \tilde{f}(\mathcal{X}). \quad (9)$$

This was a demonstration of the extension from the uncontrolled systems to the controlled systems. From now on, we will use f , and ξ interchangeably between controlled and uncontrolled systems unless otherwise stated.

Also, KO provides (approximately, in a practical settings) global linear representation for nonlinear dynamics if the right set of observable functions is chosen in as shown in the sequel. Generally speaking, the observable functions are hard to identify. They can be found by many method including, but not limited to, brute-force trial and error in a specific basis for the Hilbert space (e.g., trying numerous polynomial functions or Fourier basis functions) or by prior knowledge about the system. Several efforts have been made on this matter [27], [41]–[46] – just to name a few. **Our work rely heavily on the choice of the observable functions.** Existing literature on how to choose such dictionary of function can be utilized in order to make best use of the presented paradigm. We discuss the effect of choosing the bad lifting dictionary in illustrative example 2 in section IV.B

Motivated by the preceding analysis, we will make use of the idea of lifting the nonlinear dynamics from its state-space to look linear in a higher-dimensional state-space.

Remark 1. *Since our our method rely on the good choice of the observable functions, a blurry prior physical knowledge of the underlying plant, not necessarily a complete knowledge, but at least a knowledge that can describe the domain shape in*

which the system operates to design the observable functions could be of a great benefit. \square

Remark 2. *At this stage of the work, we design the controller directly from the data. This step requires a set of observable functions that are satisfactory to approximate KO with notes regarding that being discussed in remark 1. In the sense that we do not focus on the identification of the KO itself, we did not include discussion on such a topic. However, in more general scenarios, one may need to identify the operator for any purpose. Readers can refer to [47], [48].* \square

Now, the collected set \mathcal{D} should be revised. Instead of having the system's states only, we must consider the additional observable functions taking the form of $\Xi(x) = [\xi_1(x) \ \xi_2(x) \ \dots \ \xi_p(x)]^\top$. The observable functions $\Xi \in \mathbb{R}^p (p > n)$. Note that we only lift the state not the control. So the set \mathcal{D} becomes

$$U_0 := [u_0 \ u_1 \ \dots \ u_{T-1}] \in \mathbb{R}^{m \times T}, \quad (10a)$$

$$Z_0 := \Xi(X_0) \in \mathbb{R}^{p \times T}, \quad (10b)$$

$$Z_1 := \Xi(X_1) \in \mathbb{R}^{p \times T}. \quad (10c)$$

Remark 3. *In response to this change, a slight modification of assumption 1, where $T \geq n + m$ will be replaced by $T \geq p + m$.* \square

In response to this, the condition in (4) becomes,

$$\|e_k^\xi\| \leq \gamma \|\xi(x_k)\|, \quad (11)$$

where $e_k^\xi := \xi(x_k) - \xi(x_{k_i})$. Hence, after choosing the set of observable functions, the system in (1) can be now formulated as

$$z_{k+1} = Az_k + Bu_k, \quad (12a)$$

$$x_k = Cz_k. \quad (12b)$$

III.B EVENT-TRIGGERED CONTROL FOR THE LIFTED REPRESENTATION OF THE NON-LINEAR DYNAMICS

Let's consider the system given in (12), the globally linear version of the system in (1), subject to the controller (2) that result in

$$z_{k+1} = Az_k + BKz_{k_i} \quad (13a)$$

$$= Az_k + BKz_k + BKz_{k_i} - BKz_k \quad (13b)$$

$$= (A + BK)z_k + BKe_k, \quad \forall k \in [k_i, k_{i+1}), \quad (13c)$$

which can be understood as a closed-loop representation of the system in (12) with the state error.

An alternative representation of the event-triggered closed loop system should be derived to account for the data-driven nature of this work. In ref. [49] the authors

derived a data-driven representation of the closed loop system without considering the matrix BK . On the other hand, Digge and Pasumathy [20] arrived to a closed loop representation that allows dealing with the event-triggered formulation. The representation in [5] is modified to account for the lifted linear representation of the nonlinear dynamics.

Lemma 1 (Data-driven representation [6], [20]). *The equivalent data-driven closed loop representation of the system (13) under satisfaction of assumption 1 and where*

$$\begin{bmatrix} I \\ K \end{bmatrix} = \begin{bmatrix} Z_0 \\ U_0 \end{bmatrix} L, \text{ and } \begin{bmatrix} 0 \\ K \end{bmatrix} = \begin{bmatrix} Z_0 \\ U_0 \end{bmatrix} N, \quad (14)$$

holds is given by

$$z_{k+1} = Z_1 L z_k + Z_1 N e_k, \quad (15)$$

where L and N are $T \times p$ matrices. \square

Proof. Let assumption 1 be satisfied. Hence, by the Rouché-Capelli theorem, there exist L and N matrices that satisfy (14). So, another representation of (15) can be written as

$$z_{k+1} = \begin{bmatrix} A & B \end{bmatrix} \begin{bmatrix} I \\ K \end{bmatrix} z_k + \begin{bmatrix} A & B \end{bmatrix} \begin{bmatrix} 0 \\ K \end{bmatrix} e_k.$$

Using (14), the closed-loop system is given by

$$z_{k+1} = \underbrace{\begin{bmatrix} A & B \end{bmatrix} \begin{bmatrix} Z_0 \\ U_0 \end{bmatrix}}_{Z_1} L z_k + \underbrace{\begin{bmatrix} A & B \end{bmatrix} \begin{bmatrix} Z_0 \\ U_0 \end{bmatrix}}_{Z_1} N e_k.$$

Therefore, the data-driven representation of the closed-loop system (13) is given by (14). \square

This formulation can be considered as a reparametrization of the system in (13) in terms of data. In other words, no need for the prior explicit system identification step. Since the formulation is derived, we move forward to derive the condition for system (15) to be exponentially stable in Lyapunov sense. A linear system described by $z_{k+1} = A z_k$, where $A \in \mathbb{R}^p$, is considered exponentially stable if there exists a function $V : \mathbb{R}^p \mapsto \mathbb{R}$ defined by $V(z_k) = z_k^\top S z_k$ with $S \succ 0$ and symmetric, such that $V(z_{k+1}) \leq \alpha V(z_k)$ along the system's trajectories for all $k \geq 0$ and for some $\alpha \in \mathcal{A} =]0, 1[\in \mathbb{R}$.

Remark 4. *For unstable systems, the choice of α is critical as it impacts the values of the controller gain $K(\alpha)$ which must satisfy the necessary conditions and thresholds to stabilize the system. Mathematically we can formulate it as,*

$$\alpha^* = \inf_{\alpha \in \mathcal{A}} \{ \alpha : K(\alpha) \implies |\lambda_i| < 1, \forall \lambda_i \},$$

where the $K(\alpha)$ is the gains corresponding to one value of α on \mathcal{A} . \square

Considering a classical Lyapunov candidate function described in the later paragraph, the exponential Lyapunov stability criteria² is given by

$$\begin{bmatrix} z_k \\ e_k \end{bmatrix}^\top \begin{bmatrix} L^\top Z_1^\top S Z_1 L - \alpha S & L^\top Z_1^\top S Z_1 N \\ N^\top Z_1^\top S Z_1 L & N^\top Z_1^\top S Z_1 N \end{bmatrix} \begin{bmatrix} z_k \\ e_k \end{bmatrix} \leq 0 \quad (16)$$

In this work, the design of the ETC strategy should not violate the Lyapunov stability condition in (16) to ensure exponential stability.

III.C LEARNING CONTROLLER FROM DATA

Firstly, we design the controller gains to stabilize the globally linearized system. We consider the data-driven closed loop representation in (15) neglecting the error at this stage

$$z_{k+1} = Z_1 L z_k, \quad (17)$$

the controller gains can be designed directly from data, as discussed in [6, Section IV. A]. Further, the following theorem ensures the Lyapunov stability condition.

Theorem 1 (Direct Controller Design). *Let condition 1 hold. And by exploiting the results of lemma 1. Then any matrix G_1 that satisfy the following LMI,*

$$\begin{bmatrix} Z_0 G_1 & G_1^\top Z_1^\top \\ Z_1 G_1 & Z_0 G_1 \end{bmatrix} \succeq 0 \quad (18)$$

results in

$$K = U_0 G_1 (Z_0 G_1)^{-1} \quad (19)$$

which stabilizes the system (12). \square

Proof. To check the stability in exponential decay of the system (17) with a rate α , implies

$$L^\top Z_1 S Z_1 L - \alpha S \preceq 0, \quad (20)$$

with L satisfying (14). Let $G_1 := L S^{-1}$, and pre- and post-multiply (20) by S^{-1} , the stability of the system can be guaranteed if there exists two matrices G_1 and S such that

$$\begin{aligned} G_1^\top Z_1^\top S Z_1 G_1 - \alpha S^{-1} &\preceq 0 \\ K S^{-1} &= U_0 G_1 \\ S^{-1} &= Z_0 G_1 \end{aligned}$$

²The full analysis is given in the appendix.

Moreover, we use $S^{-1} = Z_0 G_1$ and obtain

$$\begin{aligned} G_1^\top Z_1^\top (Z_0 G_1) Z_1 G_1 - \alpha Z_0 G_1 &\preceq 0 \\ Z_0 G_1 &\succ 0 \\ K &= U_0 G_1 (Z_0 G_1)^{-1} \end{aligned}$$

Using Schur's complement lemma on the first inequality, we reach to (18) which results in gains given from (19) that exponentially stabilize the system. \square

III.D LEARNING THE TRIGGERING POLICY FROM DATA

In the interval $[k_i, k_{i+1})$, it is essential that inequality (16), which ensures exponential convergence, is also satisfied. The following theorem derives a window for the parameter γ that ensures the stability of system (15).

Theorem 2 (Optimal Threshold). *Assume that the condition 1 is satisfied. So, the relative threshold parameter γ for the event-triggered implementation (4) with the controller (19) can be calculated by solving for γ such that*

$$\begin{aligned} &\max_{q, G_2} \gamma \\ &\text{s.t.} \\ &\begin{bmatrix} \alpha Z_0 G_1 & \underline{0} & G_1^\top Z_1^\top & \gamma Z_0 G_1 \\ \underline{0} & qI & G_2^\top Z_1^\top & \underline{0} \\ Z_1 G_1 & Z_1 G_2 & Z_0 G_1 & \underline{0} \\ \gamma Z_0 G_1 & \underline{0} & \underline{0} & qI \end{bmatrix} \succeq \underline{0}, \\ &q > 0, \quad Z_0 G_2 = 0, \quad U G_2 - qK = 0, \end{aligned} \quad (21)$$

which will result in stability of the system (15) in exponential behaviour. \square

Proof. For exponential stability during event-triggered control, whenever the triggering condition (4) is met, the condition (16), which guarantees stability, must hold as well. This relationship can be encoded using the S-procedure [50]. According to the S-procedure, (4) implies (16) if there exists a constant $\eta \geq 0$ such that:

$$\eta \begin{bmatrix} -\gamma^2 I & \underline{0} \\ \underline{0} & I \end{bmatrix} \preceq \begin{bmatrix} L^\top Z_1^\top S Z_1 L - \alpha S & L^\top Z_1^\top S Z_1 L \\ L^\top Z_1^\top S Z_1 L & L^\top Z_1^\top S Z_1 L \end{bmatrix}.$$

Using Schur's complement, and post- and pre-multiplying by the $\text{diag}(S^{-1}, I, I)$, we derive:

$$\begin{bmatrix} -\eta\gamma^2 S^{-2} + \alpha S^{-1} & \underline{0} & S^{-1} L^\top Z_1^\top \\ \underline{0} & \eta I & N^\top Z_1^\top \\ Z_1 L S^{-1} & Z_1 N \eta^{-1} & S^{-1} \end{bmatrix} \succeq \underline{0}.$$

By changing the variables $G_1 = L S^{-1}$, $G_2 = \eta^{-1} N$,

$q = \eta^{-1}$, and $S^{-1} = Z_0 G_1$, we arrive at the LMI:

$$\begin{bmatrix} \alpha Z_0 G_1 & \underline{0} & G_1^\top Z_1^\top & \gamma Z_0 G_1 \\ \underline{0} & qI & G_2^\top Z_1^\top & \underline{0} \\ Z_1 G_1 & Z_1 G_2 & Z_0 G_1 & \underline{0} \\ \gamma Z_0 G_1 & \underline{0} & \underline{0} & qI \end{bmatrix} \succeq \underline{0}.$$

The result of theorem 2 allows to maximize γ over the variables G_2 and q . The result also implies that any $\gamma \in [0, \gamma^*)$ stabilizes the system, where γ^* is the solution for (21). \square

Now, we have all the components put together. A detailed algorithm for the entire process is given in algorithm 1.

Algorithm 1 Koopman Operator-Based Event-Triggered Control

Require: α , X_0 , X_1 , and U_0

- 1: Lift X_0 , and X_1 via (10 b, and c)
 - 2: Solve for G_1 in the LMI given in (18)
 - 3: Solve for the controller gain K in (19)
 - 4: Maximize the threshold parameter γ to get γ^* in (21)
 - 5: Choose any $\gamma \in [0, \gamma^*)$, (typically the max. value gives wider inter-event time window)
 - 6: **return** γ^* , and K
-

IV ILLUSTRATIVE SIMULATIONS AND RESULTS

In the following, we present three numerical examples, each serving a specific purpose detailed in the sequel. (edit: rationale behind the example to serve the proof of the concept)

Example 1 in subsection IV.A, as it allows exact linearization through an appropriate choice of the observable function, is used to examine the effect of various parameters in the proposed method. To do so, the sensitivity to the decaying parameter α is analyzed by evaluating the maximum value of the discrete derivative of the Lyapunov function. Additionally, the algorithm's ability to stabilize the system from various initial conditions is investigated.

Secondly, Example 2 in Equation IV.B serves a good one to study the effect of the choice of observable functions, as there is, to the best of the authors' knowledge, no known selection that yields a closed-form exact linearization of the system.

Finally, the third example in subsection IV.C shows the generality of the proposed method when it comes to linear systems in a sense made precise in the corresponding section.

At the end of this section, we provide additional notes regarding the proposed method.

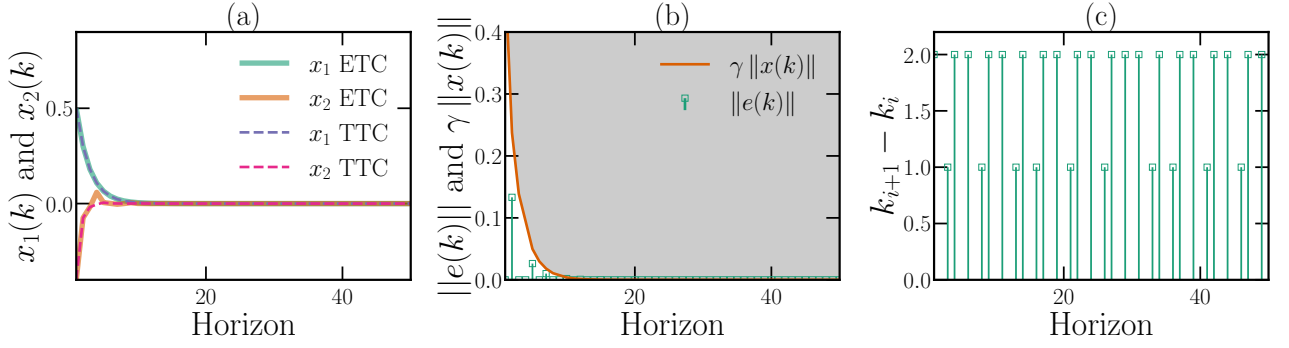


Figure 3: Results of the illustrative example 1. (a) Behaviour of state x_1 and x_2 for both ETC and TTC over the horizon. (b) Norms of the error $\|e_k\|$ and the threshold parameter $\gamma\|x_k\|$. (c) Inter-event times $k_{i+1} - k_i$ showing the intervals between successive events.

IV.A ILLUSTRATIVE EXAMPLE 1: PROOF OF CONCEPT

We consider a case of nonlinear system with slow manifold used in relative works [51]–[53]:

$$\begin{bmatrix} x_1 \\ x_2 \end{bmatrix} \mapsto \begin{bmatrix} \rho x_1 \\ \kappa x_2 + (\rho^2 - \kappa)x_1^2 + u \end{bmatrix}. \quad (22)$$

In this scenario, there exists a polynomial stable manifold defined as $x_2 = x_1^2$. Within the Koopman-inspired framework, if the correct observable functions were chosen such that $\Xi(x) = [x_1 \ x_2 \ x_1^2]^\top$, the nonlinear system in (22) can be expressed linearly as

$$\begin{bmatrix} z_1 \\ z_2 \\ z_3 \end{bmatrix}_{k+1} = \begin{bmatrix} \rho & 0 & 0 \\ 0 & \kappa & (\rho^2 - \kappa) \\ 0 & 0 & \rho^2 \end{bmatrix} \begin{bmatrix} z_1 \\ z_2 \\ z_3 \end{bmatrix}_k + \begin{bmatrix} 0 \\ 1 \\ 0 \end{bmatrix} u_k \quad (23)$$

Considering the parameters for the system, $\rho = 0.6$, and $\kappa = 1.2$, the corresponding eigenvalues are $\lambda_1 = 0.6$, $\lambda_2 = 1.2$, and $\lambda_3 = 0.36$. Since $\lambda_2 > 1$, the system exhibits instability and the goal is to stabilize the trajectory around the origin. We collected the data for $T = 45$ which is enough for assumption 1 to hold – on a theoretical note, $T \geq m + p$ samples should be enough (i.e. in this example $T \geq 4$) to obey assumption 1. Therefore, $T = 4$ should work. The input signal is drawn from a normal distribution following $u \sim \mathcal{N}(0, 1)$.

Then, after deploying the steps in algorithm 1, we obtain $K = [0.0206 \ -1.1109 \ -0.1530]$, which in turn gives $\gamma^* = 0.7664$. We simulated the system for both ETC, and TTC and illustrated the behavior in Fig. 3. All the results depicted in Fig. 3, are acquired after pulling the states back from the higher-dimensional space, in this case from \mathbb{R}^3 to \mathbb{R}^2 , by applying (12b) with $C = \begin{bmatrix} I_2 & 0 \\ 0 & 0 \end{bmatrix}$.

Fig. 3(a), illustrates the state evolution x_1 and x_2

against time under both ETC and TTC techniques. The trajectories for ETC demonstrate excellent tracking performance in comparison with the nominal TTC. This highlights the efficacy of the developed event-triggered approach in maintaining system stability while minimizing unnecessary updates.

Also, in Fig. 3(b), the graph shows that $\|e_k\|$ remains consistently below $\gamma\|x_k\|$, satisfying the triggering condition. As shown in Fig. 3(c), the substantial reduction in communication instances (40%) addresses potential concerns regarding communication overhead in practical implementations.

Finally, as noted from the numerical results, ETC not only achieves comparable performance to TTC but does so with fewer communication instances (about 40 compared to 100) and lower control cost (approximately 0.203 vs. 0.210), which supports our hypotheses. Another note in our experiment, both Koopman based linearization ETC and TTC have control cost much lower than the traditional Taylor linearization technique, consistent with the results of Brunton et al. [51].

For this example, we want to thoroughly examine and understand the influence of various parameters on the system's behavior and stability. This includes analysis of how different initial conditions and the parameter α impact the system dynamics. We explore these effects through a series of extensive simulations, designed to provide a comprehensive view of the system's response under a range of scenarios to enrich our theoretical insights and understanding.

Initially, we assessed the robustness of the algorithm by simulating ten different random initial conditions drawn from a uniform distribution $\sim \mathcal{U}(-5, 5)$. Fig. 4 shows the behavior of both x_1 and x_2 while starting with those random initial conditions. The figures show that while the initial conditions varies significantly, the be-

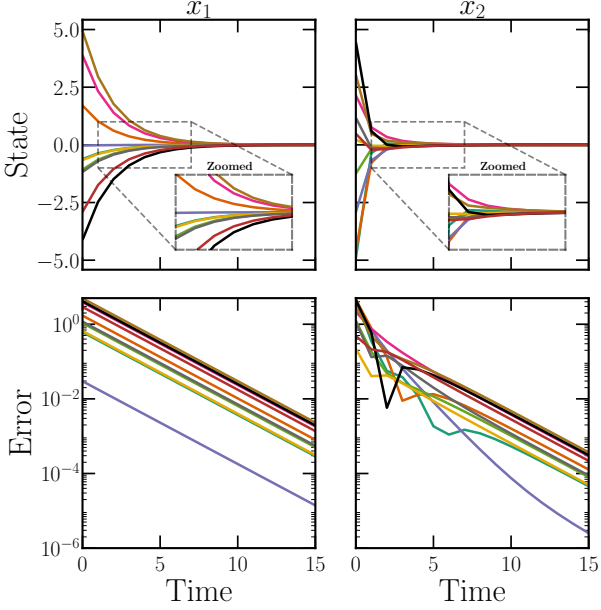


Figure 4: A simulation of ten random initial conditions drawn from a uniform distribution $X \sim \mathcal{U}(-5, 5)$. The figure shows the behaviour of x_1 (left), and x_2 (right).

haviour of the system states stabilizes in a finite amount of time. An interesting observation from the same figure is that the error decay rate between the state and the reference in the log scale is nearly linear, supporting the paper’s earlier demonstration of the exponential error decaying property.

Subsequently, the initial conditions were fixed at $x_0 = [0.5 \ -0.4]$ simulations were conducted across a fine grid of different α values ranging from 0.4 to 1. The choice of 0.4 as the starting value is informed by empirical observations, which indicate that this value represents the minimum threshold necessary to achieve an adequate gain for system stabilization, as detailed in remark 4. Fig. 5 demonstrates that for each value of α , there is no violation in the rate of Lyapunov function decay. The values on the x-axis in this figure must not exceed their corresponding values on the y-axis (i.e. they cannot cross the line $\max(V(k+1)/V(k)) = \alpha$). In other words, no deviation from the expected decaying behavior is observed.

In terms of time analysis, using a persistently excited signal sequence of length 45, the controller learning process took 0.4 seconds on an M2 MacBook Air, demonstrating the algorithm’s practical efficiency. Similarly, learning the triggering policy under the same setup was achieved in 0.49 seconds.

IV.B ILLUSTRATIVE EXAMPLE 2: POLYNOMIAL SYSTEM

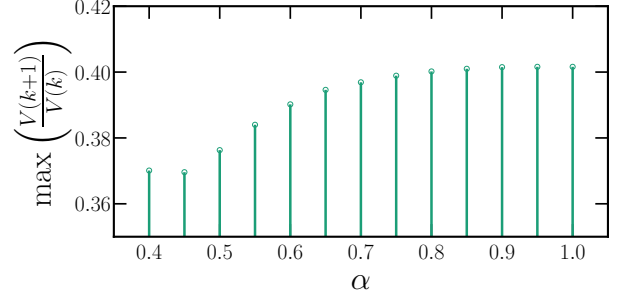


Figure 5: The relationship between α and the Lyapunov function decay rate. Simulations confirm no violations in the decay rate, as all points lie below the boundary $\max(V(k+1)/V(k)) = \alpha$, ensuring system stability across the tested α range.

In this example, we consider a discrete-time nonlinear polynomial system defined as:

$$\begin{bmatrix} x_1 \\ x_2 \end{bmatrix}_{k+1} = \begin{bmatrix} ax_1 + bx_1^2 + cx_2 \\ dx_1x_2 + ex_2^2 + u \end{bmatrix}_k, \quad (24)$$

with parameters $a = 1.05$, $b = 0.1$, $c = 0.5$, $d = 0.25$, and $e = 0.08$. For this system, data were collected for $T = 150$ which is sufficient for assumption 1 to hold. In this example, we gather the data in a closed-loop manner inspired by Ref. [54] practical guidelines. In their work, they gather the identification data using a controller architecture similar to the one intended for design. For example, in the current example, we wish to design a stabilizing controller in the form of $u = Kz$. Therefore, we adopt a closed loop controller of a similar structure, $u = \tilde{K}z$, where the over all signal is perturbed by a random signal to ensure excitation. Perturbed trajectories are generated starting from a nonzero initial condition. The choice of the observable functions are motivated by the nonlinear terms in the system plus higher order polynomials as follows: $\Xi(x) = [1 \ x_1 \ x_2 \ x_1^2 \ x_1x_2 \ x_2^2 \ x_1^3 \ x_2^3 \ x_1^3 \ x_2^3]^\top$. The addition of the higher polynomials in the dictionary of the observable functions helped to reduce the steady state error as shown in Fig. 7. With the previous parameters and the choosing observables, in addition to choosing $\alpha = 0.7$, we proceed to apply Algorithm 1. As a result, we got $K = \begin{bmatrix} -0.8742 & -0.3989 & -0.3779 & -0.5845 & -0.1581 \dots \\ \dots & 0.0301 & 0.0463 & -0.0157 & 0.0084 & -0.0071 \end{bmatrix}$, and $\gamma = 0.2237$. The corresponding results and the behavior of the system are shown in Fig. 6. Although the interpretations of these results are quiet similar to that of subsection IV.A, we still need to asses the choice of the observable functions; since the system

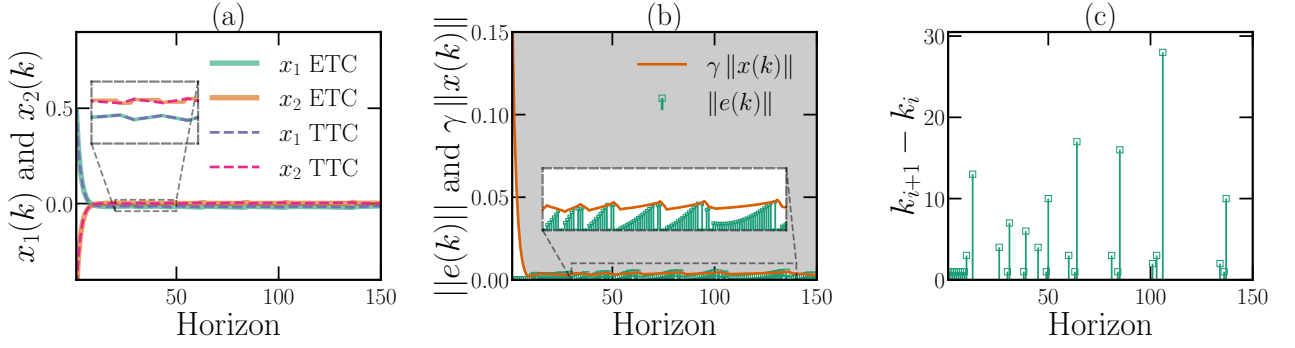


Figure 6: Results of the illustrative example 2. (a) Behaviour of state x_1 and x_2 for both ETC and TTC over the horizon. (b) Norms of the error $\|e_k\|$ and the threshold parameter $\gamma\|x_k\|$. (c) Inter-event times $k_{i+1} - k_i$ showing the intervals between successive events.

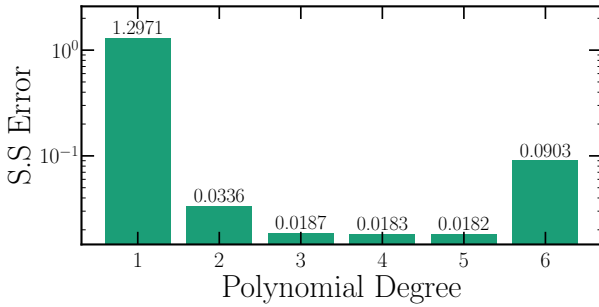


Figure 7: Steady-state error versus polynomial degree of the lifting function used for controller synthesis.

does not obey a choice of observables that exactly linearize the nonlinear system in a closed form as done in subsection IV.A. This is known as the closure problem.

To assess the effect of observable functions, we tested multiple cases under different observables. We adhere to monomial lifting functions with increasing order. Firstly, one can see the weak representation of a first-order polynomial for observable functions. This means that we implicitly assume that the nonlinear system in (24) can be well represented using linear observables, which is not evident from the first column of Fig. 7 following our understanding. Furthermore, a clear decreasing pattern appears for the steady state error as the degree number increases from 2 to 5. Surprisingly, the steady state error starts to increase at degree 6 which is a sign of overfitting. Consequently, increasing the number of observables does not guarantee a good representation. Further discussion on this will be provided in subsection V.A.

IV.C ILLUSTRATIVE EXAMPLE 3: LINEAR CASE NOTE

In this example, we consider the discrete-time linear system (originally presented in [20])

$$x_{k+1} = Ax_k + Bu_k,$$

with $x_k \in \mathbb{R}^2$ and u_k generated from a random control signal within the interval $[-3, 3]$. The system matrices are given by $A = \begin{bmatrix} 0.91 & 0.0995 \\ 0.02 & 0.99 \end{bmatrix}$, $B = \begin{bmatrix} 0.01 \\ -0.184 \end{bmatrix}$, and the simulation is performed over 20 data points to learn a controller gain K with $\alpha = 0.9$ as well as the triggering threshold γ . Under the choice of the observable functions as identity, the gain K and an event-triggering threshold γ are computed according to the framework in 1 and resulted in $K = \begin{bmatrix} 0.3820 & 0.8179 \end{bmatrix}$ and $\gamma = 0.4653$.

Notably, if the observable functions are chosen as the identity, then the algorithm directly addresses the linear dynamics without any additional lifting. In this case, our approach reduces to the classical linear control and event-triggered control framework as presented in [20]. The results of this example are depicted in Fig. 8 which matches with excellent agreement the results in Digge and Pasumarthu [20] work.

V DISCUSSIONS

V.A ON THE CHOICE OF THE OBSERVABLE FUNCTIONS

We devote this section to discussing some notes towards practical discussion of the selection of observable functions. As mentioned earlier in the paper, the choice of the lifting functions is critical part in designing the direct data driven controller that abides to an additional event-triggering role. This is also noted in the literature covering the Koopman operator [55].

The authors noted that the rate of convergence of the Koopman based identification method depends on the dictionary of the observable functions which they

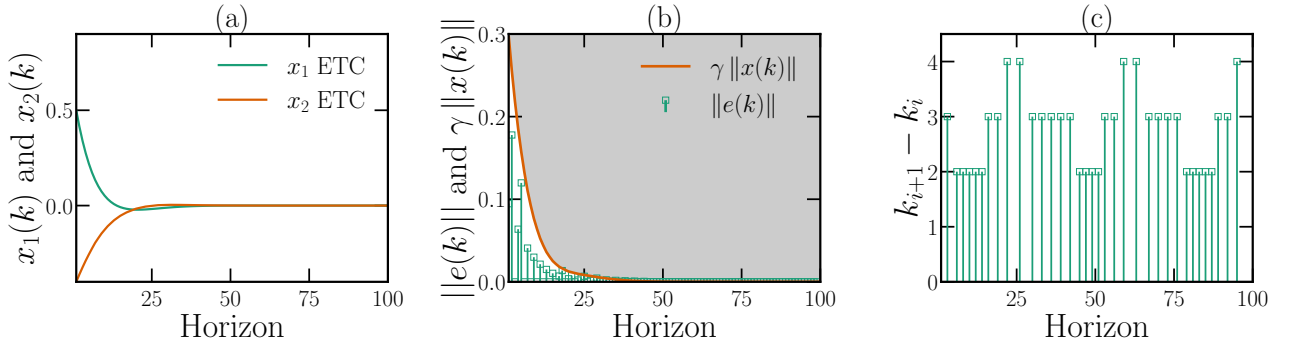


Figure 8: Results of the illustrative example 3. (a) Behaviour of state x_1 and x_2 . (b) Norms of the error $\|e_k\|$ and the threshold parameter $\gamma\|x_k\|$. (c) Inter-event times $k_{i+1} - k_i$ showing the intervals between successive events.

refer to as trials or basis functions. In their work they assume the basis functions spans the subspace of the observables. One can motivate the choice of the observables in our methods using similar approach. Possible choices of the observables are: polynomials, and Radial Basis Functions (RBFs). As advised by the authors, polynomials are a good option to be used for the system defined on \mathbb{R}^N , and the RBFs are a good candidate for systems defined on irregular domains.

Recently, many research has focused on the idea of finding a good set of observables, including: 1. employing deep learning autoencoders [43], [56], 2. local higher-order derivatives of the nonlinear system [46] (though it requires a symbolic expression of the nonlinear system), 3. motivating the choice of observables by analytical constructions in [44] and [57] specifically tailored to certain robotic systems by exploiting the topological spaces of these systems to guide the construction of Hermite polynomial-based observables, 4. avoiding explicit basis selection by defining observables implicitly in a reproducing kernel Hilbert space [58], [59] using kernel functions (e.g. Gaussian kernel $k(x, y) = e^{\|x-y\|^2/2\sigma^2}$).

Building on the above discussion, how to choose an appropriate set of observables remains an important, yet open, question. Fortunately, many of the methods discussed above have shown practical effectiveness.

V.B ON THE CONTROLLER SYNTHESIS

In this section we refer back to the examples in subsection IV.A, and Equation IV.B. Although the feedback control law looks linear on the observable space z , it could be looked to it as a nonlinear controller on the original state x . For example, the illustrative example 1 in subsection IV.A, the designed controller in terms of

the original states can be interpreted as,

$$\begin{aligned} u &= [K_1 \quad K_2] \begin{bmatrix} x_1 \\ x_2 \end{bmatrix} + K_3 x_1^2 \\ &= 0.0206 x_1 - 1.1109 x_2 - 0.1540 x_1^2 \end{aligned} \quad (25)$$

where the third term indicates the nonlinearity imposed by the choice of the nonlinear observable function x_2^2 . Similar analysis could be done for example 2 by examining the effect of the observables on the control law. On the other hand, in example 3 in subsection IV.C, the control law remains linear as it originally introduced.

We recommend that the future research should look into how to optimally design the controller gain and also a policy that respects the system stability.

VI CONCLUSION

To sum up, this study proposes an event-triggered control approach based on data-driven methods for discrete-time nonlinear systems. By lifting the nonlinear dynamics into a higher-dimensional linear representation inspired by the KO theory, the method makes it possible to create an event-triggered controller driven by data. Through the development of a closed-loop system and the implementation of a triggering strategy, the proposed method stabilizes the plant with less frequent control updates.

The event-triggered closed-loop system's exponential stability is guaranteed by the stability analysis, which is based on the Lyapunov criterion. Numerical simulations and theoretical analysis are used to show how effective the suggested strategy is. This work creates opportunities for real-world applications in networked control systems and advances event-triggered control techniques for nonlinear systems.

The foundations provided by this work shall allow dealing with many other scenarios including, when the

plant (discrete or continuous) include time varying parameters, when the full state measurements are not available, or when policies other than the zero-order hold is used. Additionally, examining the various lifting techniques available in the literature is important, as well as, testing the scalability of the solution.

A LYAPUNOV STABILITY ANALYSIS

This subsection of the appendix presents the exponential stability of the system given by

$$z_{k+1} = Z_1 L z_k + Z_1 N e_k \quad (26)$$

in a Lyapunov sense with the candidate $V(k) = z_k^\top S z_k$.

First, $V(z_{k+1})$ can be computed as follows

$$\begin{aligned} V(z_{k+1}) &= (Z_1 L z_k + Z_1 N e_k)^\top S (Z_1 L z_k + Z_1 N e_k) \\ &= z_k^\top L^\top Z_1^\top S Z_1 L z_k + z_k^\top L^\top Z_1^\top S Z_1 N e_k + \dots \\ &\dots e_k^\top N^\top Z_1^\top S Z_1 L z_k + e_k^\top N^\top Z_1^\top S Z_1 N e_k \end{aligned} \quad (27)$$

Lyapunov exponential stability condition with convergence rate α can be reached by defining $V(z_{k+1}) \leq \alpha V(z_k)$. This leads to the following identity based on the candidate Lyapunov function

$$\begin{aligned} &z_k^\top L^\top Z_1^\top S Z_1 L z_k + z_k^\top L^\top Z_1^\top S Z_1 N e_k + \dots \\ &\dots e_k^\top N^\top Z_1^\top S Z_1 L z_k + e_k^\top N^\top Z_1^\top S Z_1 N e_k \leq \alpha z_k^\top S z_k \end{aligned} \quad (28)$$

By defining $v = \begin{bmatrix} z_k \\ e_k \end{bmatrix}$, Eqn. (28) can be written in the form of $v^\top \Psi v \leq 0$, where

$$\Psi = \begin{bmatrix} L^\top Z_1^\top S Z_1 L - \alpha S & L^\top Z_1^\top S Z_1 N \\ N^\top Z_1^\top S Z_1 L & N^\top Z_1^\top S Z_1 N \end{bmatrix} \quad (29)$$

Therefore, the Lyapunov stability condition for the system can be written as

$$\begin{bmatrix} z_k \\ e_k \end{bmatrix}^\top \begin{bmatrix} L^\top Z_1^\top S Z_1 L - \alpha S & L^\top Z_1^\top S Z_1 N \\ N^\top Z_1^\top S Z_1 L & N^\top Z_1^\top S Z_1 N \end{bmatrix} \begin{bmatrix} z_k \\ e_k \end{bmatrix} \leq 0 \quad (30)$$

If condition (30) is satisfied, it then guarantees exponential stability of the system with convergence rate α .

REFERENCES

- [1] K.-E. Årzen, "A simple event-based PID controller," *IFAC Proceedings Volumes*, vol. 32, no. 2, pp. 8687–8692, 1999.
- [2] J. Eker, P. Hagander, and K.-E. Årzen, "A feedback scheduler for real-time controller tasks," *Control Engineering Practice*, vol. 8, no. 12, pp. 1369–1378, 2000.
- [3] P. Tabuada, "Event-triggered real-time scheduling of stabilizing control tasks," *IEEE Transactions on Automatic control*, vol. 52, no. 9, pp. 1680–1685, 2007.
- [4] W. P. Heemels, K. H. Johansson, and P. Tabuada, "An introduction to event-triggered and self-triggered control," in *2012 IEEE 51st IEEE conference on decision and control (cdc)*, IEEE, 2012, pp. 3270–3285.

- [5] G. R. G. da Silva, A. S. Bazanella, C. Lorenzini, and L. Campestri, "Data-driven LQR control design," *IEEE control systems letters*, vol. 3, no. 1, pp. 180–185, 2018.
- [6] C. De Persis and P. Tesi, "Formulas for data-driven control: Stabilization, optimality, and robustness," *IEEE Transactions on Automatic Control*, vol. 65, no. 3, pp. 909–924, 2019.
- [7] L. Shi and K. Karydis, "Enhancement for robustness of koopman operator-based data-driven mobile robotic systems," in *2021 IEEE International Conference on Robotics and Automation (ICRA)*, IEEE, 2021, pp. 2503–2510.
- [8] C. Folkestad, S. X. Wei, and J. W. Burdick, "Quadrotor trajectory tracking with learned dynamics: Joint koopman-based learning of system models and function dictionaries," *arXiv preprint arXiv:2110.10341*, 2021.
- [9] Y. Susuki, I. Mezic, F. Raak, and T. Hikiyara, "Applied koopman operator theory for power systems technology," *Nonlinear Theory and Its Applications, IEICE*, vol. 7, no. 4, pp. 430–459, 2016.
- [10] S. L. Brunton, J. L. Proctor, and J. N. Kutz, "Discovering governing equations from data by sparse identification of nonlinear dynamical systems," *Proceedings of the national academy of sciences*, vol. 113, no. 15, pp. 3932–3937, 2016.
- [11] Z. M. Manaa, M. R. Elbalsky, and A. M. Abdallah, "Data-driven discovery of the quadrotor equations of motion via sparse identification of nonlinear dynamics," in *AIAA SCITECH 2024 Forum*, 2024, p. 1308.
- [12] Y. X. Jiang, X. Xiong, S. Zhang, J. X. Wang, J. C. Li, and L. Du, "Modeling and prediction of the transmission dynamics of COVID-19 based on the SINDy-LM method," *Nonlinear Dynamics*, vol. 105, pp. 2775–2794, 2021, Number: 3, ISSN: 1573269X. (visited on 02/06/2023).
- [13] M. Sorokina, S. Sygletos, and S. Turitsyn, "Sparse Identification for Nonlinear Optical Communication Systems: SINO Method," *Opt. Express*, vol. 24, no. 26, p. 30 433, Dec. 2016, arXiv:1701.01650 [physics], ISSN: 1094-4087. DOI: 10.1364/OE.24.030433. [Online]. Available: <http://arxiv.org/abs/1701.01650> (visited on 02/06/2023).
- [14] B. Bhadriraju, M. S. F. Bangi, A. Narasingam, and J. S. I. Kwon, "Operable adaptive sparse identification of systems: Application to chemical processes," *en-GB, AIChE Journal*, vol. 66, no. 11, 2020, Number: 11, ISSN: 15475905. DOI: 10.1002/aic.16980. (visited on 02/06/2023).
- [15] D. Bhattacharya, L. K. Cheng, and W. Xu, "Sparse Machine Learning Discovery of Dynamic Differential Equation of an Esophageal Swallowing Robot," *en-GB, IEEE Transactions on Industrial Electronics*, vol. 67, no. 6, pp. 4711–4720, 2020, Number: 6, ISSN: 15579948. DOI: 10.1109/TIE.2019.2928239. (visited on 02/06/2023).
- [16] M. Sznajer, "Control oriented learning in the era of big data," *IEEE Control Systems Letters*, vol. 5, no. 6, pp. 1855–1867, 2020.
- [17] M. C. Campi, A. Lecchini, and S. M. Savaresi, "Virtual reference feedback tuning: A direct method for the design of feedback controllers," *Automatica*, vol. 38, no. 8, pp. 1337–1346, 2002.
- [18] M. Fliess and C. Join, "Model-free control," *International journal of control*, vol. 86, no. 12, pp. 2228–2252, 2013.
- [19] W. Liu, J. Sun, G. Wang, F. Bullo, and J. Chen, "Data-driven self-triggered control via trajectory prediction," *IEEE Transactions on Automatic Control*, vol. 68, no. 11, pp. 6951–6958, 2023.
- [20] V. Digge and R. Pasumathy, "Data-driven event-triggered control for discrete-time LTI systems," in *2022 European Control Conference (ECC)*, IEEE, 2022, pp. 1355–1360.
- [21] X. Wang, J. Berberich, J. Sun, G. Wang, F. Allgöwer, and J. Chen, "Model-based and data-driven control of event- and self-triggered discrete-time linear systems," *IEEE Transactions on Cybernetics*, 2023.
- [22] B. O. Koopman, "Hamiltonian systems and transformation in hilbert space," *Proceedings of the National Academy of Sciences*, vol. 17, no. 5, pp. 315–318, 1931.
- [23] B. O. Koopman and J. v. Neumann, "Dynamical systems of continuous spectra," *Proceedings of the National Academy of Sciences*, vol. 18, no. 3, pp. 255–263, 1932.
- [24] I. Mezić and A. Banaszuk, "Comparison of systems with complex behavior," *Physica D: Nonlinear Phenomena*, vol. 197, no. 1-2, pp. 101–133, 2004.
- [25] I. Mezić, "Spectral properties of dynamical systems, model reduction and decompositions," *Nonlinear Dynamics*, vol. 41, pp. 309–325, 2005.
- [26] D. Bruder, X. Fu, R. B. Gillespie, C. D. Remy, and R. Vasudevan, "Koopman-based control of a soft continuum manipulator under variable loading conditions," *IEEE robotics and automation letters*, vol. 6, no. 4, pp. 6852–6859, 2021.
- [27] G. Mamakoukas, M. L. Castano, X. Tan, and T. D. Murphey, "Derivative-based koopman operators for real-time control of robotic systems," *IEEE Transactions on Robotics*, vol. 37, no. 6, pp. 2173–2192, 2021.
- [28] X. Zhu, C. Ding, L. Jia, and Y. Feng, "Koopman operator based model predictive control for trajectory tracking of an omnidirectional mobile manipulator," *Measurement and Control*, vol. 55, no. 9-10, pp. 1067–1077, 2022.

- [29] N. Komeno, B. Michael, K. Kuchler, E. Anarossi, and T. Matsubara, "Deep koopman with control: Spectral analysis of soft robot dynamics," in *2022 61st Annual Conference of the Society of Instrument and Control Engineers (SICE)*, IEEE, 2022, pp. 333–340.
- [30] M. Han, J. Euler-Rolle, and R. K. Katschmann, "Desko: Stability-assured robust control with a deep stochastic koopman operator," in *International Conference on Learning Representations*, 2021.
- [31] Z. M. Manaa, A. M. Abdallah, M. A. Abido, and S. S. A. Ali, "Koopman-LQR Controller for Quadrotor UAVs from Data," *arXiv preprint arXiv:2406.17973*, 2024.
- [32] R. R. Hossain, R. Adesunkanmi, and R. Kumar, "Data-driven linear koopman embedding for networked systems: Model-predictive grid control," *IEEE Systems Journal*, 2023.
- [33] T. Markmann, M. Straat, and B. Hammer, "Koopman-based surrogate modelling of turbulent rayleigh-bénard convection," *arXiv preprint arXiv:2405.06425*, 2024.
- [34] I. Mezić, Z. Drmač, N. Črnjarić, *et al.*, "A koopman operator-based prediction algorithm and its application to covid-19 pandemic and influenza cases," *Scientific reports*, vol. 14, no. 1, p. 5788, 2024.
- [35] J. C. Willems, P. Rapisarda, I. Markovsky, and B. L. De Moor, "A note on persistency of excitation," *Systems & Control Letters*, vol. 54, no. 4, pp. 325–329, 2005.
- [36] M. Budišić, R. Mohr, and I. Mezić, "Applied koopmanism," *Chaos: An Interdisciplinary Journal of Nonlinear Science*, vol. 22, no. 4, 2012.
- [37] P. Bevanda, S. Sosnowski, and S. Hirche, "Koopman operator dynamical models: Learning, analysis and control," *Annual Reviews in Control*, vol. 52, pp. 197–212, 2021.
- [38] J. L. Proctor, S. L. Brunton, and J. N. Kutz, "Generalizing koopman theory to allow for inputs and control," *SIAM Journal on Applied Dynamical Systems*, vol. 17, no. 1, pp. 909–930, 2018.
- [39] S. Peitz, S. E. Otto, and C. W. Rowley, "Data-driven model predictive control using interpolated koopman generators," *SIAM Journal on Applied Dynamical Systems*, vol. 19, no. 3, pp. 2162–2193, 2020.
- [40] M. Korda and I. Mezić, "Linear predictors for nonlinear dynamical systems: Koopman operator meets model predictive control," *Automatica*, vol. 93, pp. 149–160, 2018.
- [41] S. E. Otto and C. W. Rowley, "Linearly recurrent autoencoder networks for learning dynamics," *SIAM Journal on Applied Dynamical Systems*, vol. 18, no. 1, pp. 558–593, 2019.
- [42] E. Yeung, S. Kundu, and N. Hodas, "Learning deep neural network representations for koopman operators of nonlinear dynamical systems," in *2019 American Control Conference (ACC)*, IEEE, 2019, pp. 4832–4839.
- [43] B. Lusch, J. N. Kutz, and S. L. Brunton, "Deep learning for universal linear embeddings of nonlinear dynamics," *Nature communications*, vol. 9, no. 1, p. 4950, 2018.
- [44] M. Netto, Y. Susuki, V. Krishnan, and Y. Zhang, "On analytical construction of observable functions in extended dynamic mode decomposition for nonlinear estimation and prediction," in *2021 American Control Conference (ACC)*, IEEE, 2021, pp. 4190–4195.
- [45] M. Kamb, E. Kaiser, S. L. Brunton, and J. N. Kutz, "Time-delay observables for koopman: Theory and applications," *SIAM Journal on Applied Dynamical Systems*, vol. 19, no. 2, pp. 886–917, 2020.
- [46] G. Mamakoukas, M. Castano, X. Tan, and T. Murphey, "Local koopman operators for data-driven control of robotic systems," in *Robotics: science and systems*, 2019.
- [47] P. J. Schmid, "Dynamic mode decomposition of numerical and experimental data," *Journal of fluid mechanics*, vol. 656, pp. 5–28, 2010.
- [48] J. L. Proctor, S. L. Brunton, and J. N. Kutz, "Dynamic mode decomposition with control," *SIAM Journal on Applied Dynamical Systems*, vol. 15, no. 1, pp. 142–161, 2016.
- [49] C. De Persis, R. Postoyan, and P. Tesi, "Event-triggered control from data," *IEEE Transactions on Automatic Control*, 2023.
- [50] S. P. Boyd and L. Vandenberghe, *Convex optimization*. Cambridge university press, 2004.
- [51] S. L. Brunton, B. W. Brunton, J. L. Proctor, and J. N. Kutz, "Koopman invariant subspaces and finite linear representations of nonlinear dynamical systems for control," *PloS one*, vol. 11, no. 2, 2016.
- [52] A. Surana and A. Banaszuk, "Linear observer synthesis for nonlinear systems using koopman operator framework," *IFAC-PapersOnLine*, vol. 49, no. 18, pp. 716–723, 2016.
- [53] A. Surana, "Koopman operator based observer synthesis for control-affine nonlinear systems," in *2016 IEEE 55th Conference on Decision and Control*, IEEE, 2016, pp. 6492–6499.
- [54] L. Do, A. Uchytil, and Z. Hurák, "Practical guidelines for data-driven identification of lifted linear predictors for control," *arXiv preprint arXiv:2408.01116*, 2024.
- [55] M. O. Williams, I. G. Kevrekidis, and C. W. Rowley, "A data-driven approximation of the koopman operator: Extending dynamic mode decomposition," *Journal of Nonlinear Science*, vol. 25, pp. 1307–1346, 2015.
- [56] J. Ge, Y. Xu, and Z. Wu, "Deep learning-based construction of koopman observable functions for power system nonlinear dynamics," in *2024 IEEE Power & Energy Society General Meeting (PESGM)*, IEEE, 2024, pp. 1–5.
- [57] L. Shi and K. Karydis, "Acd-edmd: Analytical construction for dictionaries of lifting functions in koopman operator-based nonlinear robotic systems," *IEEE Robotics and Automation Letters*, vol. 7, no. 2, pp. 906–913, 2021.
- [58] M. O. Williams, C. W. Rowley, and I. G. Kevrekidis, "A kernel-based approach to data-driven koopman spectral analysis," *arXiv preprint arXiv:1411.2260*, 2014.
- [59] J. Lee, B. Hamzi, B. Hou, H. Owahdi, G. Santin, and U. Vaidya, "Kernel methods for the approximation of the eigenfunctions of the koopman operator," *arXiv preprint arXiv:2412.16588*, 2024.